European Journal of Medicinal Chemistry 215 (2021) 113273

Contents lists available at ScienceDirect

European Journal of Medicinal Chemistry

journal homepage: http://www.elsevier.com/locate/ejmech

Design, synthesis and biological evaluation of 7*H*-pyrrolo[2,3-*d*] pyrimidine derivatives containing 1,8-naphthyridine-4-one fragment

Jianqing Zhang [a, b, 1], Pengqin Chen [a, 1], Yongli Duan [c], Hehua Xiong [d], Hongmin Li [b], Yao Zeng [b], Guang Liang [a], Qidong Tang [a, b, *], Di Wu [a, **]

[a] Chemical Biology Research Center, School of Pharmaceutical Sciences, Wenzhou Medical University, Wenzhou, 325035, PR China
[b] Jiangxi Provincial Key Laboratory of Drug Design and Evaluation, School of Pharmacy, Jiangxi Science & Technology Normal University, Nanchang, 330013, PR China
[c] School of Optoelectronic Science and Engineering, University of Electronic Science and Technology of China (UESTC), Chengdu, 610054, PR China
[d] State Key Laboratory of Natural Medicines, Key Laboratory of Drug Quality Control and Pharmacovigilance, Department of Pharmaceutical Analysis, China Pharmaceutical University, Nanjing, 210009, China

ARTICLE INFO

Article history:
Received 30 October 2020
Received in revised form
20 January 2021
Accepted 1 February 2021
Available online 9 February 2021

Keywords:
7*H*-pyrrolo[2,3-*d*]pyrimidine
1,8-Naphthyridine-4-one
Inhibitors
Activity
Synthesis
SAR

ABSTRACT

In this study, a series of pyrrolo [2,3-*d*]pyrimidine derivatives containing 1,8-naphthyridine-4-one fragment were synthesized and their biological activity were tested. Most of the target compounds displayed moderate to excellent activity against one or more cancer cell lines and low activity against human normal cell LO2 *in vitro*. The most promising compound **51**, of which the IC_{50} values were 0.66 μM, 0.38 μM and 0.44 μM against cell lines A549, Hela and MCF-7, shown more remarkable activity and better apoptosis effect than the positive control Cabozantinib. The structure-activity relationships (SARs) indicated that double-EWGs (such as R_3 = 2-Cl-4-CF_3) on the terminal phenyl rings was a key factor in improving the biological activity. In addition, the further research on compound **51** mainly included c-Met kinase activity and selectivity, concentration dependence, and molecular docking.

1. Introduction

Cancer is a major public health problem worldwide [1–3]. Global demographic characteristics predict that cancer incidence rate will continue to increase in the next few decades, with more than 20 million cancer patients annually. Traditional treatment methods (such as surgery, radiotherapy, chemotherapy) could increase the survival rate of cancer patients, but they still have many adverse reactions [4–6]. Thus, the search of novel treatment which is efficacious and effective with low side effects is imminent. With the continuous development of medical research, targeted therapy has become a prevalent method in the treatment of cancer because of its good efficacy and low side effects [7,8].

c-Met belongs to a subfamily of receptor tyrosine kinases (RTKs) encoded by the c-Met proto-oncogene, which was discovered in human osteosarcoma cell lines [9,10]. The binding of hepatocyte growth factor (HGF) to c-Met induces a series of effects, including proliferation, angiogenesis, invasion and migration, which are essential in normal physiology [11,12]. However, the abnormal activation of c-Met occurs in many types of human cancers, such as breast, liver, gastric cancers and so on [13–15]. Therefore, c-Met has garnered considerable attention for use as an anticancer drug target, giving rise to numerous investigations pertaining to c-Met kinase inhibitors with the goal of disrupting the abnormal activation of HGF/c-Met signaling pathway.

In view of how inhibitors and c-Met kinase domain bind, small-molecular c-Met kinase inhibitors are categorized into either class I or class II. Inhibitors of class I have the characteristics of small binding region and easily produce drug resistance for patients due to the mutation near the active site of c-Met [16]. In comparison, inhibitors of class II are believed to be more effective for these mutations as their binding interactions extend beyond the entry of the c-Met active site [17]. Therefore, c-Met inhibitors of class II have

* Corresponding author. Chemical Biology Research Center, School of Pharmaceutical Sciences, Wenzhou Medical University, Wenzhou, 325035, PR China.
** Corresponding author.
E-mail addresses: tangqidongcn@126.com (Q. Tang), wudi2017@wmu.edu.cn (D. Wu).
[1] These authors contribute equally to this work.

https://doi.org/10.1016/j.ejmech.2021.113273
0223-5234/

been widely studied due to their decreased level of drug resistance as well as their reduced toxicity and stronger efficacy. As shown in Fig. 1, Cabozantinib (**1**) is the first small-molecular c-Met inhibitor of class II approved by the FDA of the United States for the treatment of late-stage non-small-cell lung cancer (NSCLC) and metastatic medullary thyroid cancer [18–20]. In addition, many Cabozantinib derivatives were reported, such as Foretinib (**2**), BMS777607 (**3**) as well as compounds **4** and **5** [21,22]. Moreover, compound **6** showed excellent efficacy with IC_{50} values in the micromolar level, as demonstrated in our previous study [23].

The c-Met inhibitors of class II have similar structural characteristics, which can be illustrated by the binding pattern of Cabozantinib with c-Met protein (PDB code: 3LQ8), as shown in Fig. 2. First, moiety A was a pyridine or its analogs, providing a nitrogen atom and mainly forming hydrogen bond with Met1160. Subsequently, the central and terminal benzene rings (moiety B) located at the hydrophobic region forming weak interactions with the surrounding amino acid residues. In particular, moiety C exhibited an obvious structural characteristic, a '5-atom linker', which means six chemical bonds distance existed between the central and terminal benzene rings. The moiety C can be modified with flexible or rigid chains to form hydrogen bond donors or acceptors with the amino acid residues of c-Met (such as Lys1110 and Asp1222) in improving the activity of the compounds [15,21,23]. The space of c-Met protein around moieties A and C was large enough for further optimization of the compounds in order to improve the biological activity. While, only minor changes in the central and terminal benzene rings were available.

In this study, the pyrrolo [2,3-*d*]pyrimidine fragment was retained as moiety A based on compound **6** from our previous work, which served as an important structure in maintaining biological activity. In this regard, different substituents were introduced into moiety A so as to study the effect of hydrogen bond formation on antiproliferative potency. As reported, various 1,8-naphthyridine-4-one derivatives represented by vosaroxin (**7**) (Fig. 3) have shown excellent anticancer effects in different types of cancer. These derivatives possessed the characteristics of a high-quality hydrogen bond receptor and gained considerable attention from researchers [24–26]. According to the 3D model of Cabozantinib (Fig. 4), an intramolecular hydrogen bond (distance = 1.714 Å) between oxygen and hydrogen atoms was formed in the '5-atom linker'. Moreover, inspired by the intramolecular hydrogen bond of Cabozantinib, 1,8-naphthyridine-4-one was introduced into moiety C to further explore biological activity while maintaining the possibility of forming intramolecular hydrogen bonds between oxygen and hydrogen atoms. Finally, various substituents such as F, Cl, CF_3 and OCH_3 were introduced to the central and terminal benzene rings (moiety B) in order to explore the influence of electron cloud accumulation in the hydrophobic region on biological activity (Fig. 4). Thus, a novel series of pyrrolo [2,3-*d*]pyrimidine derivatives containing 1,8-naphthyridine-4-one fragment were designed.

2. Results and discussion

2.1. Chemistry

2.1.1. Synthesis of 3-substituted-4-((7-substituted-7H-pyrrolo[2,3-d]pyrimidin-4-yl)oxy)anilines (13a-d)

The key intermediates of 3-substituted-4-((7-substituted-7*H*-pyrrolo [2,3-*d*]pyrimidin-4-yl)oxy)anilines **13a-d** were acquired as revealed in Scheme 1. Nucleophilic substitution reaction of commercially available 4-chloro-7*H*-pyrrolo [2,3-*d*]pyrimidine **10a** or 4-chloro-7-methyl-7*H*-pyrrolo [2,3-*d*]pyrimidine **10b** and *p*-nitrophenol or 2-fluoro-4-nitrophenol (**11a-d**) gave intermediates **12a-d**, which were then reduced to obtain intermediates **13a-d** [22,27].

Reagents and conditions: (i) *p*-nitrophenol or 2-fluoro-4-nitrophenol, diphenyl oxide, 140 °C, 8 h; (ii) Fe powder, NH_4Cl (cat.), EtOH/H_2O, 85 °C, 5 h.

2.1.2. Synthesis of the target compounds of 20–51

The target compounds **20**–**51** were prepared as illustrated in Scheme 2. Here, 1-(2-chlorophenyl)ethan-1-one (**14**) and dimethyl carbonate were refluxed in toluene at 85 °C to afford intermediate **15** as an orange oily liquid [28]. The carbanion reaction of **15** with *N*,*N*-dimethylformamide dimethyl acetal (DMF-DMA) in toluene produced intermediate **16** as a light yellow liquid, which then reacted with the corresponding anilines to obtain intermediates **17a-h**. The corresponding acid chlorides **19a-h** were then obtained by hydrolysis and carboxylation of **17a-h**, which reacted with sodium hydroxide (NaOH) and oxalyl chloride, respectively [29]. The target compounds **20**–**51** were obtained at room temperature (r.t.), and the reaction of the anilines **13a-d** with the acid chlorides **19a-h** were facilitated by *N*,*N*-diisopropylethylamine (DIPEA) in dichloromethane.

Reagents and conditions: (i) NaH, dimethyl carbonate, toluene, 85 °C, 6 h; (ii) DMF-DMA, toluene, 100 °C, 2 h; (iii) corresponding anilines, Cs_2CO_3, toluene, 150 °C, 6 h; (iv) NaOH, 1,4-dioxane, H_2O, 100 °C, 2 h; (v) oxalyl chloride, CH_2Cl_2, r. t., 0.5 h; (vi) corresponding anilines, DIPEA, CH_2Cl_2, r. t., 1 h.

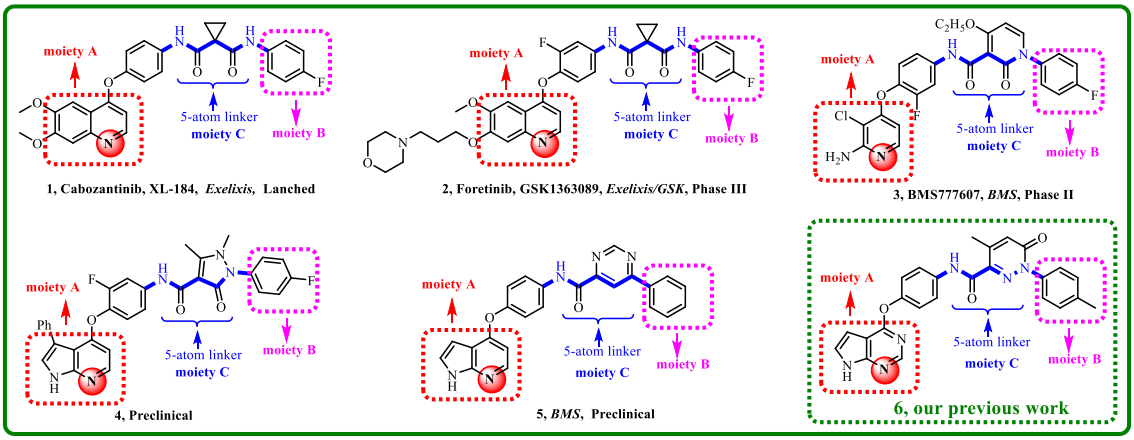

Fig. 1. The representative small-molecular c-Met kinase inhibitors from others work (**1**–**5**) and our previous work (**6**).

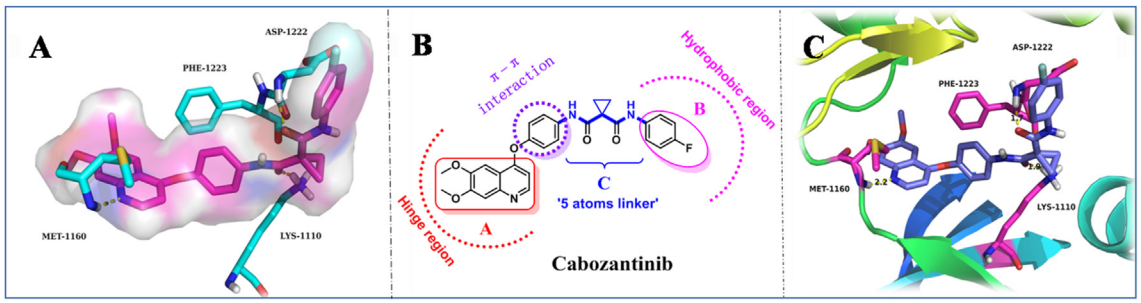

Fig. 2. Analysis of the binding mode of Cabozantinib and c-Met kinase (PDB code: 3LQ8): (A) Cavity diagram of the docking results of Cabozantinib; (B) Chemical structure of Cabozantinib and its depicted binding mode with c-Met kinase; (C) Ribbon map of the docking results of Cabozantinib. Hydrogen bonding interactions were indicated with yellow dotted line.

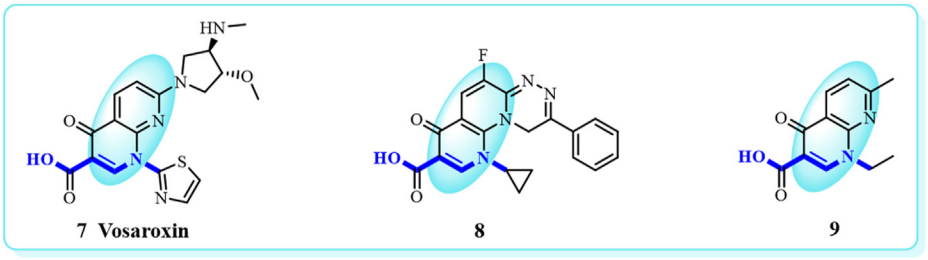

Fig. 3. Anticancer agents with 1,8-naphthyridine-4-one fragment (**7**–**9**).

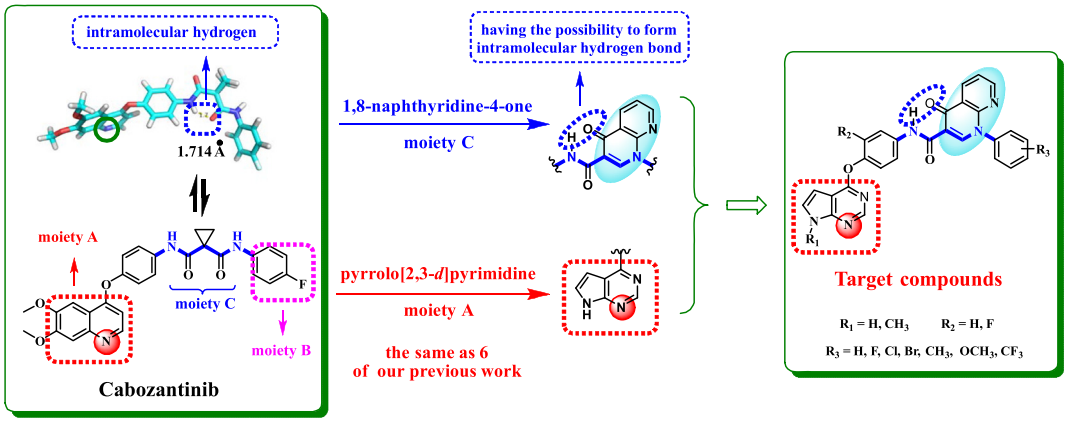

Fig. 4. The design strategy for the pyrrolo [2,3-*d*]pyrimidine derivatives with 1,8-naphthyridine-4-one fragment.

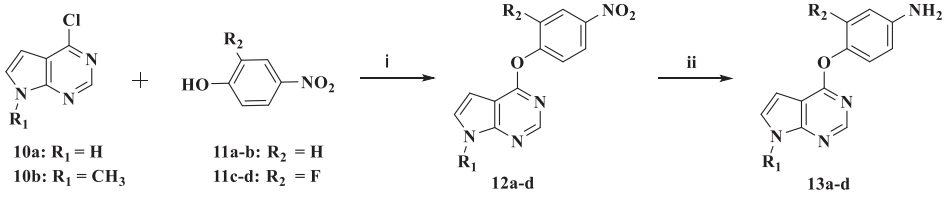

Scheme 1. Synthetic route of the key intermediates **13a-d**.

2.2. Biological evaluation

2.2.1. In vitro cytotoxic activities and SARs

The synthesized compounds (**20**–**51**) were evaluated for cytotoxicity via MTT assay against three cancer cell lines including A549 (non-small cell lung cancer cells), Hela (cervical cancer cells) and MCF-7 (breast cancer cells). Cabozantinib was used as a positive control, and the results were expressed as half-maximal inhibitory concentration (IC_{50}) values, as presented in Table 1.

Among them, A549 and Hela are high and moderate expressing cell lines of c-Met kinase, respectively, and were used to test the cytotoxic activity in our study. Although there is no overexpression

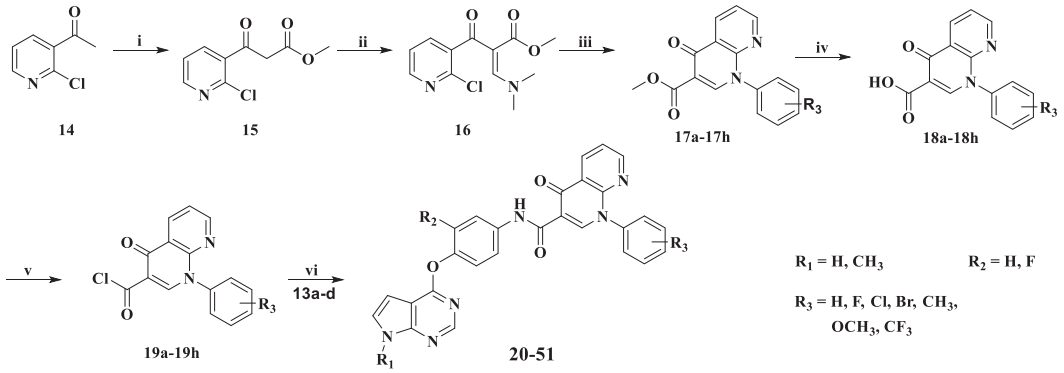

Scheme 2. Synthetic route of the target compounds.

Table 1
Structures and cytotoxic activities of the target compounds **20**–**51** against A549, Hela and MCF-7 cancer cell lines *in vitro*.

Compd.	R_1	R_2	R_3	IC_{50}[a] (μM)		
				A549	Hela	MCF-7
20	CH_3	H	4-H	2.89 ± 0.54	6.31 ± 0.82	3.62 ± 0.72
21	CH_3	H	2-F-4-Br	7.05 ± 0.23	1.46 ± 0.29	4.41 ± 0.79
22	CH_3	H	4-Br	7.34 ± 0.54	3.46 ± 0.53	9.24 ± 0.62
23	CH_3	H	4-Cl	**0.75 ± 0.15**	3.12 ± 0.65	3.47 ± 0.09
24	CH_3	H	4-F	**0.79 ± 0.02**	NA[b]	1.29 ± 0.03
25	CH_3	H	3-Cl-4-F	**0.81 ± 0.03**	2.18 ± 0.43	**0.35 ± 0.04**
26	CH_3	H	4-OCH_3	0.97 ± 0.01	9.38 ± 0.25	NA
27	CH_3	H	2-Cl-4-CF_3	3.67 ± 0.88	NA	4.27 ± 0.81
28	CH_3	F	4-H	1.89 ± 0.03	12.09 ± 2.01	11.09 ± 1.23
29	CH_3	F	2-F-4-Br	5.24 ± 0.33	NA	6.49 ± 1.17
30	CH_3	F	4-Br	1.01 ± 0.02	3.16 ± 0.43	9.24 ± 0.33
31	CH_3	F	4-Cl	6.28 ± 0.79	1.23 ± 0.33	2.12 ± 0.16
32	CH_3	F	4-F	**0.69 ± 0.02**	1.54 ± 0.25	**0.46 ± 0.01**
33	CH_3	F	3-Cl-4-F	**0.73 ± 0.01**	**0.34 ± 0.03**	NA
34	CH_3	F	4-OCH_3	5.14 ± 0.11	1.43 ± 0.54	2.81 ± 0.49
35	CH_3	F	2-Cl-4-CF_3	0.81 ± 0.11	3.25 ± 0.13	1.25 ± 0.23
36	H	F	4-H	0.93 ± 0.17	1.26 ± 0.29	4.07 ± 0.51
37	H	F	2-F-4-Br	0.89 ± 0.02	3.12 ± 0.63	2.71 ± 0.43
38	H	F	4-Br	**0.78 ± 0.01**	1.29 ± 0.03	3.65 ± 0.71
39	H	F	4-Cl	1.27 ± 0.23	**0.30 ± 0.02**	1.69 ± 0.03
40	H	F	4-F	**0.72 ± 0.04**	**0.33 ± 0.01**	0.69 ± 0.03
41	H	F	3-Cl-4-F	**0.69 ± 0.04**	NA	**0.34 ± 0.02**
42	H	F	4-OCH_3	5.85 ± 0.32	1.34 ± 0.07	4.53 ± 0.61
43	H	F	2-Cl-4-CF_3	1.32 ± 0.02	**0.25 ± 0.03**	2.45 ± 0.36
44	H	H	4-H	1.18 ± 0.02	0.65 ± 0.02	**0.09 ± 0.09**
45	H	H	2-F-4-Br	2.14 ± 0.04	**0.14 ± 0.01**	0.65 ± 0.02
46	H	H	4-Br	0.87 ± 0.01	0.51 ± 0.03	0.52 ± 0.03
47	H	H	4-Cl	3.71 ± 0.28	1.21 ± 0.24	0.76 ± 0.12
48	H	H	4-F	**0.77 ± 0.01**	**0.29 ± 0.03**	0.51 ± 0.02
49	H	H	3-Cl-4-F	NA	0.35 ± 0.02	2.11 ± 0.23
50	H	H	4-OCH_3	1.15 ± 0.24	1.65 ± 0.09	**0.46 ± 0.09**
51	H	H	2-Cl-4-CF_3	**0.66 ± 0.03**	0.38 ± 0.03	**0.44 ± 0.04**
Cabozantinib[c]				0.76 ± 0.05	0.32 ± 0.01	0.45 ± 0.04

[a] Bold type showed that the IC_{50} value of the target compound was lower than that of the positive control.
[b] NA: Not determined.
[c] Used as the positive control.

of c-Met in MCF-7 cell line, we chose it to investigate whether these compounds showed potent cytostatic activity against cells that c-Met expressed lowly [30–32].

Overall, all tested compounds showed moderate to excellent cytotoxic activity against different cancer cells. Fifteen of these compounds were more potent than Cabozantinib against one or more cancer cell lines, which further indicated that the introduction of the 1,8-naphthyridine-4-one fragment to the '5-atom linker' (moiety C) was an effective optimization strategy. Notably, as illustrated in Table 1, most target compounds were found to be more potent against A549, such as the representative compounds **23** (IC_{50} = 0.75 ± 0.15 μM), **24** (IC_{50} = 0.79 ± 0.02 μM), **25** (IC_{50} = 0.81 ± 0.03 μM), **48** (IC_{50} = 0.77 ± 0.01 μM), **51** (IC_{50} = 0.66 ± 0.03 μM). The most promising compound **51** demonstrated excellent activity against A549, Hela and MCF-7 cell lines with IC_{50} values of 0.66, 0.38 and 0.44 μM, respectively, which was more active than that of the positive control Cabozantinib.

The data listed in Table 1 showed that compounds substituted with a hydrogen atom (R_1 group) on moiety A were more active than those substituted with methyl. For instance, compound **46** (A549 IC_{50} = 0.87 μM; R_1 = H, R_2 = H, R_3 = 4-Br) had superior activity compared to compound **22** (A549 IC_{50} = 7.34 μM; R_1 = CH_3,

R_2 = H, R_3 = 4-Br), and the same trend was observed in compounds **20/44**, **24/48**, **30/38**, **31/39**. Afterward, the anticancer activity of the central benzene ring substituted by F/H atom of the linker connecting A and C was investigated, which showed that the introduction of R_2 on the central phenyl ring had no significant effect on activity, such as compounds **42** and **50**.

Further analysis revealed that compounds with different substituents of R_3 on the terminal phenyl ring (moiety B) showed different cytotoxic activity. Among them, the activity of the compounds was found to be significantly reduced when the 4-position of the terminal benzene ring was replaced by a single electron-donating group. For example, the IC_{50} value of compound **36** was 0.93 μM against A549, while compound **42** with a single electron-donating group (EDG) methoxy substituted had an IC_{50} value of 5.85 μM. Compared to R_3 substituted by EDG, compounds substituted by electron-withdrawing groups (EWGs) exhibited better activity than the lead compound (Cabozantinib), such as **23**, **25**, **26,** and so forth. Interestingly, the introduction of double electron-withdrawing groups (double-EWGs) to R_3 on the terminal phenyl ring demonstrated better activity than that of single-electron-withdrawing groups (single-EWGs). For example, when substituents were introduced to the C-2 and C-4 positions of the terminal phenyl ring (moiety B), the cytotoxic activity of **46** (R_3 = 4-Br, IC_{50} = 0.87 μM) and **48** (R_3 = 4-F, IC_{50} = 0.77 μM) was found to be 1.34 times to 1.16 times weaker than that of **51** (R_3 = 2-Cl-4-CF_3, IC_{50} = 0.66 μM). Accordingly, the results showed that the cytotoxicity of compounds with double-EWGs on the terminal benzene ring was higher than that of other substituents.

As shown in Table 2, the promising compounds exhibited excellent cytotoxicity against A549, Hela and MCF-7 cells were screened for toxicity test on normal human liver cell line LO2 via MTT assay. The results showed that the compounds had lower activity against normal cell line LO2 than that of Cabozantinib, and far lower than that of cancer cells, which indicated that the compounds had certain selectivity on cancer cells. Then, combined with the results of cytotoxicity test of Tables 1 and 2, we selected the most promising compound **51** with the excellent activity against cancer cells and low activity on normal cells to further study.

2.2.2. The relationship between the concentration of compound *51* and the cytotoxicity of three cancer cell lines

In order to effectively examine the relationship between inhibition rate and concentration, the cells were treated with seven different concentrations of compound **51** via MTT, as shown in Fig. 5. Unsurprisingly, the results demonstrated that compound **51** inhibited the growth of the three tumor cell lines in a dose-dependent manner.

Table 2
Cytotoxic activity of selected compounds against normal human liver cell line LO2 *in vitro*.

Compd.	R_1	R_2	R_3	IC_{50} (μM)
				LO2
23	CH_3	H	4-Cl	>100
24	CH_3	H	4-F	>100
25	CH_3	H	3-Cl-4-F	>100
33	CH_3	F	3-Cl-4-F	>100
38	H	F	4-Br	>100
39	H	F	4-Cl	>100
40	H	F	4-F	87.58 ± 1.94
43	H	F	2-Cl-4-CF_3	74.16 ± 1.46
44	H	H	4-H	>100
45	H	H	2-F-4-Br	>100
50	H	H	4-OCH_3	>100
51	H	H	2-Cl-4-CF_3	67.43 ± 1.25
Cabozantinib[a]				54.97 ± 0.39

[a] Used as the positive control.

2.2.3. Morphological changes of A549 cells under an inverted microscope and fluorescence microscope

In order to further explore the apoptotic mechanism of compound **51**, the morphological changes of A549 cells were monitored using an acridine orange (AO) assay. According to Fig. 6, cells in the control group (Fig. 6A) were stained with AO, presenting as an oval cell shape with a clear edge in a tight and orderly arrangement with no abnormalities. However, when the cells were treated with compound **51** at a concentration of 1.1 μM and AO staining (Fig. 6B), the cells' morphology was observed to be abnormal with evidence of cell nucleus splitting and dispersion and the RNA fragments was stained with Orange. The corresponding findings showed that compound **51** could induce apoptosis in A549 cells.

2.2.4. Apoptosis results analysis

The mechanism of A549 apoptosis induced by compound **51** was further revealed by annexin V/PI staining [23]. As shown in Fig. 7, compared to the control group, compound **51** was seen to significantly increase early apoptosis (20.05%), and its induction effect was better than that of Cabozantinib (19.87%). In addition, the advanced apoptosis rate of compound **51** was found to be higher than that of Cabozantinib. The corresponding results showed that target compound **51** could induce apoptosis of A549 cells, which was observed to be superior to that of Cabozantinib.

2.2.5. Tyrosine kinases assays

To examine the selectivity of compound **51** on c-Met over other kinases, compound **51** was screened against c-Met and six other tyrosine kinases (Table 3). At a concentration of 10 μM, the inhibition rate on c-Met of compound **51** reached 86.3%, while the inhibition rates on the six other enzymes, including PDGFR-β, Flt-3, Ron, KDR, c-Kit and ALK, were all between 23.6 and 38.0%. The results indicated that compound **51** exhibited selectivity on c-Met over other kinases.

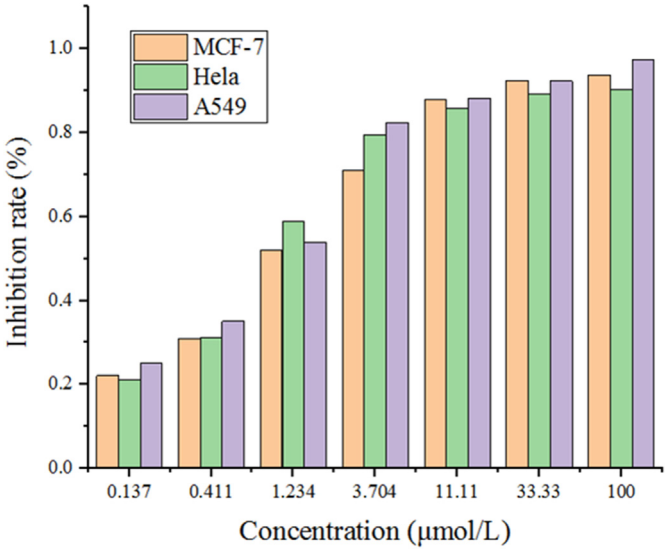

Fig. 5. The relationship between activity and concentration of selected compound **51** against our cancer cell lines.

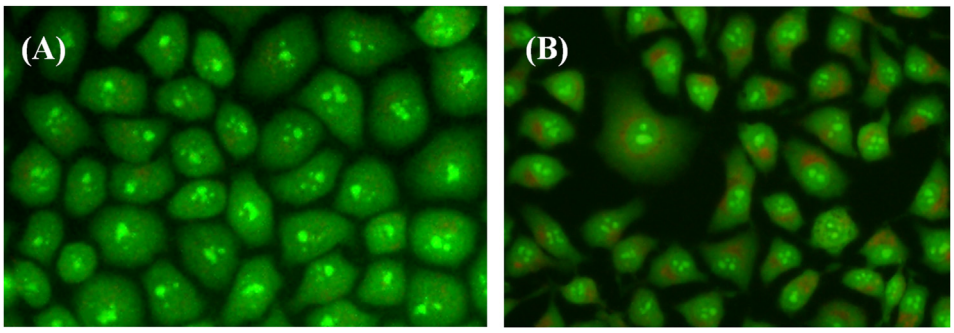

Fig. 6. The morphological changes of A549 cells were observed under inverted microscope and fluorescence microscope. (A) Blank control group; (B) the experimental group was treated with compound **51** with a concentration of 1.1 μM.

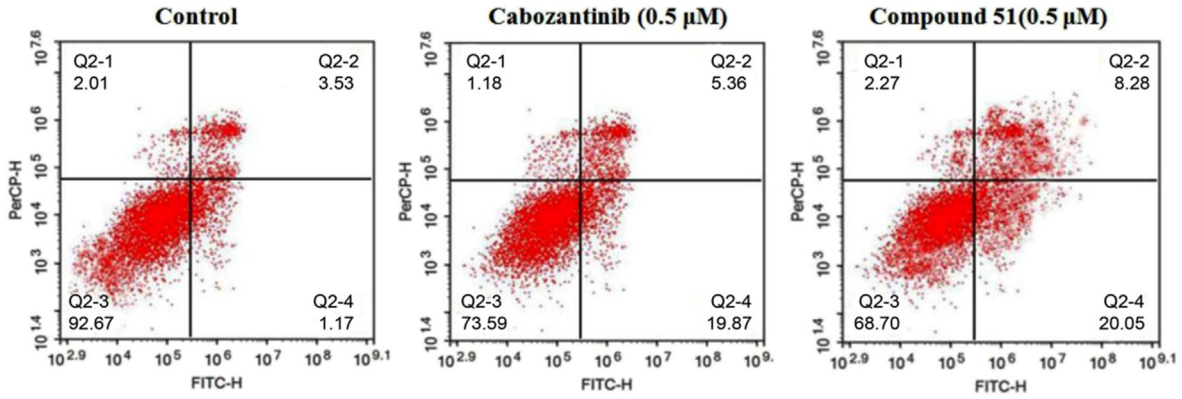

Fig. 7. Representative dot plot of Annexin V (x-axis) versus PI (y-axis) analyses. Q2-1: Mechanical damage; Q2-2: Late apoptotic and death; Q2-3: Living cells; Q2-4: Early apoptotic.

Table 3
Inhibition rates of tyrosine kinases by compound **51**.

Kinases	Inhibition rates (%)
c-Met	86.3
PDGFR-β	38.0
Flt-3	36.0
RON	30.7
KDR	30.4
c-Kit	29.7
ALK	23.6

2.3. Binding model analysis

To further elucidate the binding modes of target compounds with the active site of c-Met, molecular docking simulation studies were carried out using AutoDock vina 1.1.2. Considerable research has shown that c-Met inhibitors of class II penetrate the protein cavity with a linear stretch configuration and form a primary hydrogen bond with a pharmacodynamic effect through the aromatic ring of the hinge region and Met1160 [33,34]. The binding mode of Cabozantinib with c-Met protein (PDB ID code: 3LQ8) showed that a large enough cavity existed around the '5-atom linker' (moiety C) to accommodate the rigid segment (Fig. 8A). Interestingly, the docking study demonstrated that the 1,8-naphthyridine-4-one fragment in compound **51** could be well accommodated to the cavity, as shown in Fig. 8B and C. In addition, two nitrogen atoms of pyrrolo [2,3-*d*]pyrimidine formed a bidentate hydrogen bond with Met1160, and the amide and 1,8-naphthyridine-4-one fragment of moiety C formed two hydrogen bonds with residues Lys1110 and Asp1222, respectively. In general, the molecular docking study showed that pyrrolo [2,3-*d*]pyrimidine derivatives containing 1,8-naphthyridine-4-one fragment could act synergistically to interact with the binding site of c-Met, and 1,8-naphthyridine-4-one fragment may serve as an effective scaffold in building a novel series of c-Met inhibitors.

3. Conclusions

In summary, pyrrolo [2,3-*d*]pyrimidine derivatives containing 1,8-naphthyridine-4-one fragment were designed and synthesized, and the cytotoxic potency against three cancer cell lines (A549, Hela and MCF-7) were evaluated. Among them, most of target compounds were more potent against one or more cancer cell lines and showed lower activity against normal human liver cell line LO2 than Cabozantinib. In particular, compound **51** showed remarkable cytotoxic activities with IC_{50} values of 0.66 μM, 0.38 μM and 0.44 μM against A549, Hela and MCF-7 cell lines, respectively. Notably, compound **51** had a better apoptosis effect than that of Cabozantinib against A549 cells. The preliminary studies on enzymatic activity revealed that compound **51** showed selectivity on c-Met over six other tyrosine kinases. Moreover, the SARs and docking studies indicated that double-EWGs (such as R_3 = 2-Cl-4-CF_3) on the terminal phenyl rings was a key factor in improving the biological activity.

4. Experimental

4.1. General information

All melting points of the target compounds were obtained using a Büchi melting point B-540 instrument (BüchiLabor technik, Flavil,

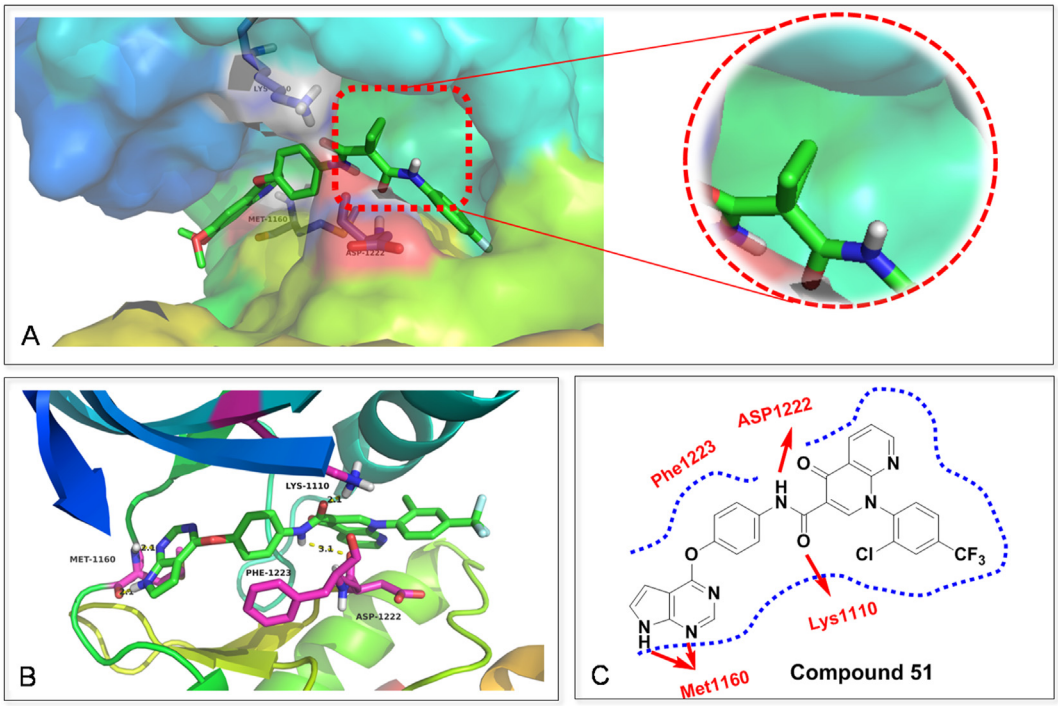

Fig. 8. Docking diagram of Cabozantinib and compound **51** with c-Met protein (PDB ID code: 3LQ8). (A) docking cavity diagram and a partial enlarged drawing of Cabozantinib; (B) 3D interaction map between the **51** and c-Met; (C) 2D interaction map between the **51** and c-Met.

Switzerland) without correction. The structures of the target compounds were determined using ^{1}H NMR, ^{13}C NMR and MS with Bruker 400 MHz or 500 MHz spectrometers (Bruker Bioscience, Billerica, MA, USA) in conjunction with tetramethylsilane (TMS) as an internal standard. Unless otherwise stated, all materials were purchased from commercial suppliers and used without purification, and the yields were not optimized.

*4.2. Synthesis of 3-substituted-4-((7-substituted-7H-pyrrolo[2,3-d] pyrimidin-4-yl)oxy)anilines **(13a-d)***

The preparation of the key intermediates **13a-d** was illustrated in detail in previous study [22,27], hence, the synthesis procedure was omitted here.

*4.2.1. 4-((7H-pyrrolo[2,3-d]pyrimidin-4-yl)oxy)aniline (**13a**)*

Brown solid; yield: 55.6%; m. p.: 185.1–186.2 °C; ^{1}H NMR (400 MHz, DMSO-d_6) δ 12.12 (s, 1H), 8.27 (s, 1H), 7.38 (d, J = 3.1 Hz, 1H), 6.88 (d, J = 8.6 Hz, 2H), 6.60 (d, J = 8.5 Hz, 2H), 6.24 (d, J = 3.3 Hz, 1H), 5.07 (s, 2H). ESI-MS: m/z 226.1 [M+H] $^{+}$.

*4.2.2. 4-((7H-pyrrolo[2,3-d]pyrimidin-4-yl)oxy)-3-fluoroaniline (**13b**)*

Gray solid; yield: 56.1%; m. p.: 177.4–180.1 °C; ^{1}H NMR (400 MHz, DMSO-d_6) δ 12.17 (s, 1H), 8.27 (s, 1H), 7.38 (s, 1H), 6.88 (d, J = 8.7 Hz, 2H), 6.60 (d, J = 8.7 Hz, 2H), 6.24 (d, J = 3.1 Hz, 1H), 5.07 (s, 1H). ESI-MS: m/z 244.1 [M+H] $^{+}$.

*4.2.3. 4-((7-methyl-7H-pyrrolo[2,3-d]pyrimidin-4-yl)oxy)aniline (**13c**)*

White solid; yield: 56.8%; m. p.: 170.5–172.2 °C; ^{1}H NMR (400 MHz, DMSO-d_6) δ 8.32 (s, 1H), 7.46 (d, J = 3.4 Hz, 1H), 6.97 (d, J = 8.5 Hz, 2H), 6.77 (d, J = 8.6 Hz, 3H), 6.31 (d, J = 3.3 Hz, 2H), 3.36 (s, 3H). ESI-MS: m/z 240.1 [M+H] $^{+}$.

*4.2.4. 3-fluoro-4-((7-methyl-7H-pyrrolo[2,3-d]pyrimidin-4-yl)oxy) aniline (**13d**)*

Light yellow solid; yield: 59.2%; m. p.: 185.1–187.2 °C; ^{1}H NMR (400 MHz, DMSO-d_6) δ 8.32 (s, 1H), 7.50 (d, J = 3.4 Hz, 1H), 7.35 (s, 1H), 7.23 (s, 1H), 6.99 (d, J = 8.9 Hz, 1H), 6.47 (s, 1H), 5.47 (s, 2H), 3.38 (s, 3H). ESI-MS: m/z 258.1 [M+H] $^{+}$.

*4.3. General procedure for the preparation of compounds **20–51***

O-chloroacetophenone **14** (0.16 mol) and NaH (0.54 mol) were dissolved in toluene (50 mL) in an ice bath for 0.5 h. After dimethyl carbonate (0.48 mol) was slowly added into the reaction mixture, the reaction temperature was raised to 85 °C and stirred for 6 h. Following the reaction, the reaction system was cooled to r. t. and adjusted to pH = 7 with glacial acetic acid. Finally, the organic layer was concentrated to obtain intermediate **15**.

The key intermediate **15** (0.22 mol) and DMF-DMA (0.56 mol) were sequentially dissolved to toluene (75 mL) and stirred at 100 °C for 2 h. The reaction mixture was then extracted with CH_2Cl_2. The combined organic layers were washed with saturated sodium chloride solution, dried over Na_2SO_4, filtered and concentrated under reduced pressure to produce intermediate **16**.

Afterward, intermediate **16** (0.14 mol), the appropriate anilines (0.43 mol) and Cs_2CO_3 (0.1 mol) were dissolved in toluene (85 mL) and stirred at 150 °C for 6 h until TLC displayed completion of the reaction. Finally, the precipitate was collected by filtration and dried to give the corresponding intermediates **17a-h**, which were pale-yellow solids.

Key intermediates **17a-h** (15 mol) and NaOH (35 mol) were then added into the mixture solvent of 1,4-dioxane (35 mL) and water (35 mL), and the reaction mixture was heated to 100 °C. The mixture was refluxed for 2 h, after which the solution was evaporated and adjusted to pH = 4 with the addition of 10% HCl aq. A large amount of solid was aspirated, and the precipitate was collected via filtration and then dried in order to obtain the

corresponding key intermediates **18a-h**.

*4.3.1. 4-oxo-1-phenyl-1,4-dihydro-1,8-naphthyridine-3-carboxylic acid (**18a**)*

Yellow solid, yield: 67.5%; ^{1}H NMR (400 MHz, DMSO-d_6) δ 14.52 (s, 1H), 8.86 (s, 2H), 8.81 (d, J = 8.0 Hz, 1H), 7.73 (dd, J = 7.9, 4.7 Hz, 1H), 7.66 (br, 5H).

*4.3.2. 1-(4-bromo-2-fluorophenyl)-4-oxo-1,4-dihydro-1,8-naphthyridine-3-carboxylic acid (**18b**)*

Brown solid, yield: 60.5%; ^{1}H NMR (400 MHz, DMSO-d_6) δ 14.29 (s, 1H), 9.11 (s, 1H), 8.89 (s, 1H), 8.81 (d, J = 8.0 Hz, 1H), 7.92 (d, J = 9.3 Hz, 1H), 7.75 (d, J = 7.1 Hz, 2H), 7.70 (d, J = 8.6 Hz, 1H).

*4.3.3. 1-(4-bromophenyl)-4-oxo-1,4-dihydro-1,8-naphthyridine-3-carboxylic acid (**18c**)*

Brown solid, yield: 65.8%; ^{1}H NMR (400 MHz, DMSO-d_6) δ 15.10 (s, 1H), 9.21 (s, 1H), 8.82 (s, 1H), δ 8.75 (t, J = 9.7 Hz, 2H), 7.82 (d, J = 8.6 Hz, 2H), 7.61 (t, J = 8.1 Hz, 2H).

*4.3.4. 1-(4-chlorophenyl)-4-oxo-1,4-dihydro-1,8-naphthyridine-3-carboxylic acid (**18d**)*

White solid, yield: 50.6%; ^{1}H NMR (400 MHz, DMSO-d_6) δ 14.49 (s, 1H), 8.92 (s, 1H), 8.87 (s, 1H), 8.81 (d, J = 8.0 Hz, 1H), 7.74 (dd, J = 7.9, 4.5 Hz, 1H), 7.69 (br, 4H).

*4.3.5. 1-(4-fluorophenyl)-4-oxo-1,4-dihydro-1,8-naphthyridine-3-carboxylic acid (**18e**)*

Yellow solid, yield: 70.9%; ^{1}H NMR (400 MHz, DMSO-d_6) δ 14.52 (s, 1H), 8.91 (s, 1H), 8.88 (d, J = 3.5 Hz, 1H), 8.81 (d, J = 7.9 Hz, 1H), 7.76 (br, 3H), 7.46 (t, J = 8.6 Hz, 2H).

*4.3.6. 1-(3-chloro-4-fluorophenyl)-4-oxo-1,4-dihydro-1,8-naphthyridine-3-carboxylic acid (**18f**)*

Yellow solid, yield: 55.6%; ^{1}H NMR (400 MHz, DMSO-d_6) δ 14.46 (s, 1H), 9.01 (s, 1H), 8.89 (s, 1H), 8.82 (s, 1H), 8.03 (d, J = 6.3 Hz, 1H), 7.77 (br, 3H).

*4.3.7. 1-(4-methoxyphenyl)-4-oxo-1,4-dihydro-1,8-naphthyridine-3-carboxylic acid (**18g**)*

White solid, yield: 58.4%; ^{1}H NMR (400 MHz, DMSO-d_6) δ 14.57 (s, 1H), 8.88 (s, 1H), 8.85 (br, 2H), 7.73 (dd, J = 7.4, 4.2 Hz, 1H), 7.55 (d, J = 8.1 Hz, 2H), 7.14 (d, J = 8.2 Hz, 2H), 3.86 (s, 3H).

*4.3.8. 1-(2-chloro-4-(trifluoromethyl)phenyl)-4-oxo-1,4-dihydro-1,8-naphthyridine-3-carboxylic acid (**18h**)*

Yellow solid; yield: 60.5%; ^{1}H NMR (400 MHz, DMSO-d_6) δ 14.67 (s, 1H), 9.01 (s, 1H), 8.60 (s, 1H), 8.55 (d, J = 7.8 Hz, 1H), 8.05 (d, J = 8.3 Hz, 1H), 7.78 (d, J = 8.5 Hz, 2H), 7.48 (d, J = 7.7 Hz, 1H).

The reaction of oxalyl chloride and key intermediates **18a-h** (4 mol) was carried out to obtain the corresponding intermediates **19a-h**. The appropriate anilines **13a-d** (2 mol) and DIPEA (6 mol) were dissolved in dichloromethane (25 mL) to form system I. Secondly, **19a-h** obtained by acylation of **18a-h** with oxalyl chloride as acylating agent, were dissolved in anhydrous dichloromethane (20 mL) to form system II. Finally, the mixed solution of system II was dropped into system I, and stirred in an ice bath for 1 h. Finally, the mixture was removed under reduced pressure to get a crude product which was purified by column chromatography on silica gel using CH_2Cl_2: MeOH 15:1 to give the target compounds **20**–**51** as a pale yellow solid.

*4.3.9. N-(4-((7-methyl-7H-pyrrolo[2,3-d]pyrimidin-4-yl)oxy) phenyl)-4-oxo-1-phenyl-1,4-dihydro-1,8-naphthyridine-3-carboxamide (**20**)*

Yellow solid, yield: 67.8%; m. p.: 198.8–200.6 °C; ^{1}H NMR (400 MHz, DMSO-d_6) δ 12.16 (s, 1H), 8.89 (s, 1H), 8.83 (d, J = 7.9 Hz, 2H), 8.35 (s, 1H), 7.83 (d, J = 8.5 Hz, 2H), 7.73 (br, 6H), 7.52 (s, 1H), 7.28 (d, J = 8.5 Hz, 2H), 6.50 (s, 1H), 3.83 (s, 3H). ^{13}C NMR (100 MHz, DMSO-d_6) δ 178.37, 175.15, 163.79, 163.51, 155.75, 155.16, 154.05, 152.19, 151.15, 150.60, 137.98, 137.75, 131.52 (2C), 131.36, 129.76 (2C), 124.53 (3C), 123.47, 123.00 (2C), 118.08, 114.05, 103.68, 102.17, 99.51, 33.27. Anal. Calcd. for $C_{28}H_{20}N_6O_3$ (%): C, 68.84; H, 4.13; N, 17.20; Found (%): C, 68.80; H, 4.10; N, 17.12. ESI-MS: m/z 488.2 [M+H] $^+$.

*4.3.10. 1-(4-bromo-2-fluorophenyl)-N-(4-((7-methyl-7H-pyrrolo [2,3-d]pyrimidin-4-yl)oxy)phenyl)-4-oxo-1,4-dihydro-1,8-naphthyridine-3-carboxamide (**21**)*

Yellow solid, yield: 57.4%; m. p.: 233.8–234.6 °C; ^{1}H NMR (400 MHz, DMSO-d_6) δ 12.03 (s, 1H), 9.04 (s, 1H), 8.85 (s, 2H), 8.36 (s, 1H), 7.95 (s, 2H), 7.83 (d, J = 8.1 Hz, 4H), 7.73 (s, 2H), 7.53 (s, 1H), 7.28 (d, J = 8.5 Hz, 3H), 3.83 (s, 3H). Anal. Calcd. for $C_{28}H_{18}BrFN_6O_3$ (%): C, 57.45; H, 3.10; Br, 13.65; F, 3.25; N, 14.36; Found (%): C, 57.40; H, 3.11; N, 14.31. ESI-MS: m/z 584.1 [M+H] $^+$.

*4.3.11. 1-(4-bromophenyl)-N-(4-((7-methyl-7H-pyrrolo[2,3-d] pyrimidin-4-yl)oxy)phenyl)-4-oxo-1,4-dihydro-1,8-naphthyridine-3-carboxamide (**22**)*

Yellow solid, yield: 71.8%; m. p.: 223.3–224.1 °C; ^{1}H NMR (400 MHz, DMSO-d_6) δ 12.13 (s, 1H), 8.84 (dd, J = 7.6, 6.5 Hz, 3H), 8.35 (s, 2H), 7.84 (d, J = 5.1 Hz, 2H), 7.65 (d, J = 7.9 Hz, 1H), 7.52 (s, 2H), 7.27 (d, J = 8.7 Hz, 3H), 6.50 (s, 1H), 3.83 (s, 3H). Anal. calcd. for $C_{28}H_{19}BrN_6O_3$ (%): C, 59.27; H, 3.38; Br, 14.08; N, 14.81; Found (%): C, 59.26; H, 3.37; N, 14.80. ESI-MS: m/z 566.1 [M+H] $^+$.

*4.3.12. 1-(4-chlorophenyl)-N-(4-((7-methyl-7H-pyrrolo[2,3-d] pyrimidin-4-yl)oxy)phenyl)-4-oxo-1,4-dihydro-1,8-naphthyridine-3-carboxamide (**23**)*

Yellow solid, yield: 76.7%; m. p.: 233.3–234.1 °C; ^{1}H NMR (400 MHz, DMSO-d_6) δ 12.14 (s, 1H), 8.91 (s, 1H), 8.82 (s, 1H), 8.36 (s, 1H), 7.83 (d, J = 8.6 Hz, 3H), 7.72 (br, 5H), 7.52 (s, 1H), 7.28 (d, J = 8.8 Hz, 2H), 6.51 (s, 1H), 3.83 (s, 3H). ^{13}C NMR (100 MHz, DMSO-d_6) δ 176.90, 161.70, 161.60, 153.63, 152.50, 150.10, 149.82, 149.03, 148.49, 139.22, 135.91, 135.65, 133.89, 129.73 (2C), 129.37 (2C), 129.27, 122.44 (2C), 122.05, 120.88 (2C), 112.12, 104.73, 97.41, 31.18. Anal. calcd. for $C_{28}H_{19}ClN_6O_3$ (%): C, 64.31; H, 3.66; Cl, 6.78; N, 16.07; Found (%): C, 64.30; H, 3.65; N, 16.08. ESI-MS: m/z 522.1 [M+H] $^+$.

*4.3.13. 1-(4-fluorophenyl)-N-(4-((7-methyl-7H-pyrrolo[2,3-d] pyrimidin-4-yl)oxy)phenyl)-4-oxo-1,4-dihydro-1,8-naphthyridine-3-carboxamide (**24**)*

Yellow solid, yield: 66.5%; m. p.: 254.3–256.1 °C; ^{1}H NMR (400 MHz, DMSO-d_6) δ 12.15 (s, 1H), 8.90 (s, 1H), 8.84 (s, 1H), 8.82 (s, 1H), 8.36 (s, 2H), 7.83 (d, J = 8.7 Hz, 2H), 7.74 (d, J = 8.5 Hz, 3H), 7.53 (br, 1H), 7.48 (s, 1H), 7.28 (d, J = 7.9 Hz, 2H), 6.51 (s, 1H), 3.83 (s, 3H). ^{13}C NMR (100 MHz, DMSO-d_6) δ 176.88, 163.28, 161.69, 161.64, 159.66 (d, J = 226.0 Hz), 153.62, 152.52, 150.09, 149.16, 148.52, 136.68, 135.87, 135.66, 134.92, 130.08, 129.99, 129.25, 122.40, 122.11, 121.38, 120.89, 120.28, 116.27 (d, J = 13 Hz), 116.04 (d, J = 12 Hz), 112.03, 104.75, 97.40, 31.17.^{19}F NMR (471 MHz, DMSO-d_6) δ −112.05. Anal. calcd. for $C_{28}H_{19}FN_6O_3$ (%): C, 66.40; H, 3.78; F, 3.75; N, 16.59; Found (%): C, 66.42; H, 3.77; N, 16.58. ESI-MS: m/z 506.2 [M+H] $^+$.

*4.3.14. 1-(3-chloro-4-fluorophenyl)-N-(4-((7-methyl-7H-pyrrolo [2,3-d]pyrimidin-4-yl)oxy)phenyl)-4-oxo-1,4-dihydro-1,8-naphthyridine-3-carboxamide (**25**)*

Yellow solid, yield: 56.5%; m. p.: 234.3–236.1 °C; ^{1}H NMR (400 MHz, DMSO-d_6) δ 12.13 (s, 1H), 8.96 (s, 1H), 8.85 (s, 1H), 8.35 (d, J = 7.4 Hz, 2H), 7.94 (s, 1H), 7.82 (s, 3H), 7.53 (s, 2H), 7.27 (s, 3H), 7.15 (s, 1H), 3.83 (s, 3H). ^{13}C NMR (100 MHz, DMSO-d_6) δ 177.34, 162.20, 162.06, 159.04, 154.18, 153.00, 152.62, 150.73, 149.80 (d, J = 160 Hz), 148.40, 148.15, 131.03, 129.78, 122.95, 122.65, 122.56, 122.35, 122.24, 121.79, 121.39, 120.92, 120.70, 117.91 (d, J = 32 Hz), 114.77, 112.62, 105.23, 97.90, 31.68.^{19}F NMR (471 MHz, DMSO-d_6) δ −116.09. Anal. calcd. for $C_{28}H_{18}ClFN_6O_3$ (%): C, 62.17; H, 3.35; Cl, 6.55; F, 3.51; N, 15.54; Found (%): C, 62.16; H, 3.36; N, 15.55. ESI-MS: m/z 540.1 [M+H] $^+$.

*4.3.15. 1-(4-methoxyphenyl)-N-(4-((7-methyl-7H-pyrrolo[2,3-d] pyrimidin-4-yl)oxy)phenyl)-4-oxo-1,4-dihydro-1,8-naphthyridine-3-carboxamide (**26**)*

Yellow solid, yield: 50.5%; m. p.: 245.3–246.1 °C; ^{1}H NMR (400 MHz, DMSO-d_6) δ 12.18 (s, 1H), 8.87 (s, 1H), 8.82 (d, J = 6.1 Hz, 2H), 8.36 (s, 1H), 7.83 (d, J = 8.7 Hz, 2H), 7.59 (s, 1H), 7.57 (s, 1H), 7.53 (s, 2H), 7.28 (d, J = 8.2 Hz, 2H), 7.15 (d, J = 8.6 Hz, 2H), 6.50 (s, 1H), 3.83 (s, 3H). ^{13}C NMR (100 MHz, DMSO-d_6) δ 176.78, 161.72, 159.56, 153.64, 152.46, 150.09, 149.37, 148.41, 135.83, 135.69, 133.24, 129.28, 128.83 (2C), 122.47 (2C), 122.19, 121.91, 121.40, 120.84 (2C), 114.47 (2C), 111.76, 104.69, 97.40, 55.55, 31.19. Anal. calcd. for $C_{29}H_{22}N_6O_4$ (%): C, 67.17; H, 4.28; N, 16.21; Found (%): C, 67.16; H, 4.27; N, 16.20. ESI-MS: m/z 518.2 [M+H] $^+$.

*4.3.16. 1-(2-chloro-4-(trifluoromethyl)phenyl)-N-(4-((7-methyl-7H-pyrrolo[2,3-d]pyrimidin-4-yl)oxy)phenyl)-4-oxo-1,4-dihydro-1,8-naphthyridine-3-carboxamide (**27**)*

Yellow solid, yield: 56.1%; m. p.: 234.3–236.1 °C; ^{1}H NMR (400 MHz, DMSO-d_6) δ 12.03 (s, 1H), 9.04 (s, 1H), 8.85 (s, 1H), 8.36 (s, 2H), 7.97 (s, 2H), 7.83 (d, J = 8.9 Hz, 3H), 7.74 (s, 1H), 7.53 (s, 1H), 7.29 (s, 2H), 6.51 (s, 1H), 3.83 (s, 3H). Anal. calcd. for $C_{29}H_{18}ClF_3N_6O_3$ (%): C, 58.94; H, 3.07; Cl, 6.00; F, 9.64; N, 14.22; Found (%): C, 58.83; H, 3.08; N, 14.21. ESI-MS: m/z 590.1 [M+H] $^+$.

*4.3.17. N-(3-fluoro-4-((7-methyl-7H-pyrrolo[2,3-d]pyrimidin-4-yl) oxy)phenyl)-4-oxo-1-phenyl-1,4-dihydro-1,8-naphthyridine-3-carboxamide (**28**)*

Yellow solid, yield: 65.1%; m. p.: 234.3–235.1 °C; ^{1}H NMR (400 MHz, DMSO-d_6) δ 12.28 (s, 1H), 8.90 (s, 1H), 8.84 (s, 1H), 8.83 (s, 1H), 8.36 (s, 1H), 8.02 (s, 1H), 7.98 (d, J = 7.3 Hz, 1H), 7.66 (s, 1H), 7.64 (s, 1H), 7.62 (s, 1H), 7.58 (d, J = 7.3 Hz, 2H), 7.53 (s, 1H), 7.45 (s, 1H), 6.65 (t, J = 8.1 Hz, 2H), 3.85 (s, 3H). Anal. calcd. for $C_{28}H_{19}FN_6O_3$ (%): C, 66.40; H, 3.78; F, 3.75; N, 16.59; Found (%): C, 66.41; H, 3.73; N, 16.58. ESI-MS: m/z 506.2 [M+H] $^+$.

*4.3.18. 1-(4-bromo-2-fluorophenyl)-N-(3-fluoro-4-((7-methyl-7H-pyrrolo[2,3-d]pyrimidin-4-yl)oxy)phenyl)-4-oxo-1,4-dihydro-1,8-naphthyridine-3-carboxamide (**29**)*

Yellow solid, yield: 70.4%; m. p.: 205.3–207.1 °C; ^{1}H NMR (400 MHz, DMSO-d_6) δ 12.14 (s, 1H), 9.06 (s, 1H), 8.84 (s, 1H), 8.36 (s, 2H), 7.97 (d, J = 7.0 Hz, 2H), 7.80 (s, 2H), 7.73 (s, 1H), 7.58 (s, 2H), 6.65 (s, 2H), 3.85 (s, 3H). Anal. calcd. for $C_{28}H_{17}BrF_2N_6O_3$ (%): C, 55.74; H, 2.84; Br, 13.24; F, 6.30; N, 13.93; Found (%): C, 55.73; H, 2.83; N, 13.92. ESI-MS: m/z 602.1 [M+H] $^+$.

*4.3.19. 1-(4-bromophenyl)-N-(3-fluoro-4-((7-methyl-7H-pyrrolo [2,3-d]pyrimidin-4-yl)oxy)phenyl)-4-oxo-1,4-dihydro-1,8-naphthyridine-3-carboxamide (**30**)*

Yellow solid, yield: 60.5%; m. p.: 245.3–247.1 °C; ^{1}H NMR (400 MHz, DMSO-d_6) δ 12.26 (s, 1H), 8.92 (s, 1H), 8.83 (d, J = 6.1 Hz, 1H), 8.40 (s, 1H), 8.35 (d, J = 8.7 Hz, 1H), 7.84 (d, J = 8.5 Hz, 2H), 7.65 (d, J = 8.6 Hz, 3H), 7.60 (s, 1H), 7.59 (s, 1H), 7.57 (d, J = 6.4 Hz, 2H), 7.53 (d, J = 5.1 Hz, 2H), 3.85 (s, 3H). Anal. calcd. for $C_{28}H_{18}BrFN_6O_3$ (%): C, 57.45; H, 3.10; Br, 13.65; F, 3.25; N, 14.36; Found (%): C, 57.44; H, 3.11; N, 14.35. ESI-MS: m/z 584.1 [M+H] $^+$.

*4.3.20. 1-(4-chlorophenyl)-N-(3-fluoro-4-((7-methyl-7H-pyrrolo [2,3-d]pyrimidin-4-yl)oxy)phenyl)-4-oxo-1,4-dihydro-1,8-naphthyridine-3-carboxamide (**31**)*

Yellow solid, yield: 55.6%; m. p.: 245.3–246.1 °C; ^{1}H NMR (400 MHz, DMSO-d_6) δ 12.26 (s, 1H), 8.91 (s, 1H), 8.84 (s, 1H), 8.82 (s, 1H), 8.36 (s, 1H), 7.73 (br, 4H), 7.57 (s, 2H), 7.47 (s, 2H), 7.46 (s, 1H), 6.64 (s, 1H), 3.85 (s, 3H). Anal. calcd. for $C_{28}H_{18}ClFN_6O_3$ (%): C, 62.17; H, 3.35; Cl, 6.55; F, 3.51; N, 15.54; Found (%): C, 67.16; H, 3.34; N, 15.55. ESI-MS: m/z 540.1 [M+H] $^+$.

*4.3.21. N-(3-fluoro-4-((7-methyl-7H-pyrrolo[2,3-d]pyrimidin-4-yl) oxy)phenyl)-1-(4-fluorophenyl)-4-oxo-1,4-dihydro-1,8-naphthyridine-3-carboxamide (**32**)*

Yellow solid, yield: 70.6%; m. p.: 225.3–226.1 °C; ^{1}H NMR (400 MHz, DMSO-d_6) δ 12.25 (s, 1H), 8.92 (s, 1H), 8.82 (s, 1H), 8.39 (d, J = 7.4 Hz, 1H), 8.36 (s, 1H), 7.71 (s, 3H), 7.69 (s, 1H), 7.60 (s, 2H), 7.58 (s, 1H), 7.52 (s, 1H), 6.65 (s, 1H), 3.86 (s, 3H). Anal. calcd. for $C_{28}H_{18}F_2N_6O_3$ (%): C, 64.12; H, 3.46; F, 7.24; N, 16.02; Found (%): C, 64.11; H, 3.45; N, 16.01. ESI-MS: m/z 524.1 [M+H] $^+$.

*4.3.22. 1-(3-chloro-4-fluorophenyl)-N-(3-fluoro-4-((7-methyl-7H-pyrrolo[2,3-d]pyrimidin-4-yl)oxy)phenyl)-4-oxo-1,4-dihydro-1,8-naphthyridine-3-carboxamide (**33**)*

Yellow solid, yield: 60.7%; m. p.: 215.3–216.1 °C; ^{1}H NMR (400 MHz, DMSO-d_6) δ 12.23 (s, 1H), 8.97 (s, 1H), 8.83 (d, J = 8.0 Hz, 1H), 8.35 (s, 1H), 8.07 (d, J = 7.5 Hz, 1H), 7.99 (d, J = 7.8 Hz, 1H), 7.79 (br, 4H), 7.55 (dd, J = 7.8, 6.0 Hz, 3H), 7.48 (s, 1H), 6.64 (d, J = 7.5 Hz, 1H), 3.85 (s, 3H). Anal. calcd. for $C_{28}H_{17}ClF_2N_6O_3$ (%): C, 60.17; H, 3.07; Cl, 6.34; F, 6.80; N, 15.04; Found (%): C, 60.16; H, 3.06; N, 15.03. ESI-MS: m/z 558.1 [M+H] $^+$.

*4.3.23. N-(3-fluoro-4-((7-methyl-7H-pyrrolo[2,3-d]pyrimidin-4-yl) oxy)phenyl)-1-(4-methoxyphenyl)-4-oxo-1,4-dihydro-1,8-naphthyridine-3-carboxamide (**34**)*

Yellow solid, yield: 63.2%; m. p.: 205.3–206.1 °C; ^{1}H NMR (400 MHz, DMSO-d_6) δ 12.30 (s, 1H), 8.87 (s, 1H), 8.83 (s, 1H), 8.39 (s, 1H), 8.36 (s, 1H), 8.01 (s, 1H), 7.98 (s, 1H), 7.79 (s, 1H), 7.61 (s, 2H), 7.57 (s, 2H), 7.17 (s, 1H), 7.14 (s, 1H), 6.69 (d, J = 7.9 Hz, 1H), 6.65 (s, 1H), 3.86 (s, 3H), 3.84 (s, 3H). Anal. calcd. for $C_{29}H_{21}FN_6O_4$ (%): C, 64.92; H, 3.95; F, 3.54; N, 15.66; Found (%): C, 64.91; H, 3.94; N, 15.65. ESI-MS: m/z 536.2 [M+H] $^+$.

*4.3.24. 1-(2-chloro-4-(trifluoromethyl)phenyl)-N-(3-fluoro-4-((7-methyl-7H-pyrrolo[2,3-d]pyrimidin-4-yl)oxy)phenyl)-4-oxo-1,4-dihydro-1,8-naphthyridine-3-carboxamide (**35**)*

Yellow solid, yield: 75.2%; m. p.: 203.3–206.1 °C; ^{1}H NMR (400 MHz, DMSO-d_6) δ 12.13 (s, 1H), 9.05 (s, 1H), 8.84 (s, 1H), 8.36 (s, 1H), 8.01 (s, 1H), 7.98 (s, 1H), 7.94 (s, 1H), 7.92 (s, 1H), 7.79 (d, J = 7.3 Hz, 1H), 7.73 (s, 2H), 7.57 (s, 2H), 6.64 (s, 1H), 3.85 (s, 3H). Anal. calcd. for $C_{29}H_{17}ClF_4N_6O_3$ (%): C, 57.20; H, 2.81; Cl, 5.82; F, 12.48; N, 13.80; Found (%): C, 57.21; H, 2.82; N, 13.82. ESI-MS: m/z 608.1 [M+H] $^+$.

*4.3.25. N-(4-((7H-pyrrolo[2,3-d]pyrimidin-4-yl)oxy)-3-fluorophenyl)-4-oxo-1-phenyl-1,4-dihydro-1,8-naphthyridine-3-carboxamide (**36**)*

Yellow solid, yield: 44.5%; m. p.: 225.3–226.1 °C; ^{1}H NMR (400 MHz, DMSO-d_6) δ 12.27 (s, 1H), 8.90 (s, 1H), 8.84 (s, 2H), 8.29 (s, 1H), 8.01 (s, 1H), 7.98 (s, 1H), 7.70 (br, 6H), 7.52 (s, 3H), 6.60 (s,

1H). Anal. calcd. for $C_{27}H_{17}FN_6O_3$ (%): C, 65.85; H, 3.48; F, 3.86; N, 17.07; Found (%): C, 65.84; H, 3.47; N, 17.06. ESI-MS: *m/z* 492.1 $[M+H]^+$.

4.3.26. N-(4-((7H-pyrrolo[2,3-d]pyrimidin-4-yl)oxy)-3-fluorophenyl)-1-(4-bromo-2-fluorophenyl)-4-oxo-1,4-dihydro-1,8-naphthyridine-3-carboxamide (**37**)

Yellow solid, yield: 57.5%; m. p.: 225.3–226.1 °C; ^{1}H NMR (400 MHz, DMSO-d_6) δ 12.32 (s, 1H), 12.14 (s, 1H), 9.06 (s, 1H), 8.83 (d, *J* = 7.9 Hz, 2H), 8.31 (s, 1H), 7.94 (dd, *J* = 7.6, 8.8 Hz, 2H), 7.81 (d, *J* = 7.8 Hz, 1H), 7.73 (s, 2H), 7.52 (s, 2H), 7.45 (d, *J* = 7.8 Hz, 1H), 6.62 (s, 1H). ^{13}C NMR (100 MHz, DMSO-d_6) δ 176.97, 161.65, 160.88, 158.38, 154.96 (d, *J* = 179 Hz), 154.71 (d, *J* = 228 Hz), 152.59, 149.98, 149.41, 149.23, 136.82 (d, *J* = 10 Hz), 136.07, 135.27 (d, *J* = 13 Hz), 131.24, 128.61, 127.13 (d, *J* = 13 Hz), 125.54, 124.66, 123.31 (d, *J* = 9 Hz), 122.41, 121.11, 120.01, 119.78, 116.16, 112.55, 108.27 (d, *J* = 14 Hz), 104.07, 97.79. Anal. calcd. for $C_{27}H_{15}BrF_2N_6O_3$ (%): C, 55.03; H, 2.57; Br, 13.56; F, 6.45; N, 14.26; Found (%): C, 55.02; H, 2.56; N, 14.27. ESI-MS: *m/z* 588.0 $[M+H]^+$.

4.3.27. N-(4-((7H-pyrrolo[2,3-d]pyrimidin-4-yl)oxy)-3-fluorophenyl)-1-(4-bromophenyl)-4-oxo-1,4-dihydro-1,8-naphthyridine-3-carboxamide (**38**)

Yellow solid, yield: 56.5%; m. p.: 225.3–226.1 °C; ^{1}H NMR (400 MHz, DMSO-d_6) δ 12.25 (s, 1H), 8.92 (s, 1H), 8.84 (s, 1H), 8.82 (s, 1H), 8.29 (s, 1H), 8.00 (d, *J* = 7.8 Hz, 1H), 7.85 (s, 1H), 7.83 (s, 1H), 7.65 (d, *J* = 8.3 Hz, 3H), 7.52 (s, 3H), 6.61 (s, 1H). Anal. calcd. for $C_{27}H_{16}BrFN_6O_3$ (%): C, 56.76; H, 2.82; Br, 13.98; F, 3.33; N, 14.71; Found (%): C, 56.75; H, 2.81; N, 14.70. ESI-MS: *m/z* 570.0 $[M+H]^+$.

4.3.28. N-(4-((7H-pyrrolo[2,3-d]pyrimidin-4-yl)oxy)-3-fluorophenyl)-1-(4-chlorophenyl)-4-oxo-1,4-dihydro-1,8-naphthyridine-3-carboxamide (**39**)

Yellow solid, yield: 55.2%; m. p.: 204.3–207.1 °C; ^{1}H NMR (400 MHz, DMSO-d_6) δ 12.31 (s, 1H), 12.25 (s, 1H), 8.92 (s, 1H), 8.83 (s, 2H), 8.31 (s, 1H), 7.99 (s, 2H), 7.72 (br, 5H), 7.53 (s, 2H), 6.62 (s, 1H). ^{13}C NMR (100 MHz, DMSO-d_6) δ 177.38, 162.46, 161.38, 154.19, 154.08, 151.79 (d, *J* = 268 Hz), 150.34, 149.71, 139.67, 137.41 (d, *J* = 10 Hz), 136.40, 135.71 (d, *J* = 13 Hz), 134.42, 130.23 (2C), 129.87 (2C), 126.07, 125.20, 122.63, 121.87, 116.59, 112.30, 108.87, 108.64, 104.56, 98.30. Anal. calcd. for $C_{27}H_{16}ClFN_6O_3$ (%): C, 61.55; H, 3.06; Cl, 6.73; F, 3.61; N, 15.95; Found (%): C, 61.54; H, 3.05; N, 15.96. ESI-MS: *m/z* 526.1 $[M+H]^+$.

4.3.29. N-(4-((7H-pyrrolo[2,3-d]pyrimidin-4-yl)oxy)-3-fluorophenyl)-1-(4-fluorophenyl)-4-oxo-1,4-dihydro-1,8-naphthyridine-3-carboxamide (**40**)

Yellow solid, yield: 62.1%; m. p.: 220.3–221.1 °C; ^{1}H NMR (400 MHz, DMSO-d_6) δ 12.31 (s, 1H), 12.26 (s, 1H), 8.91 (s, 1H), 8.84 (s, 2H), 8.31 (s, 1H), 7.98 (s, 1H), 7.73 (s, 3H), 7.55 (br, 5H), 6.62 (s, 1H). ^{13}C NMR (100 MHz, DMSO-d_6) δ 176.86, 163.30, 161.98, 160.89, 154.37 (d, *J* = 221 Hz), 154.02 (d, *J* = 203 Hz), 152.61, 149.98 (2C), 149.38, 136.96, 136.65, 135.86, 130.09 (2C), 130.00, 125.55, 124.68, 122.06, 121.38, 116.34, 116.11 (2C), 111.70, 108.26 (d, *J* = 23 Hz), 104.07, 97.80.^{19}F NMR (471 MHz, DMSO-d_6) δ −104.52, −113.10. Anal. calcd. for $C_{27}H_{16}F_2N_6O_3$ (%): C, 63.53; H, 3.16; F, 7.44; N, 16.46; Found (%): C, 63.52; H, 3.15; N, 16.45. ESI-MS: *m/z* 510.1 $[M+H]^+$.

4.3.30. N-(4-((7H-pyrrolo[2,3-d]pyrimidin-4-yl)oxy)-3-fluorophenyl)-1-(3-chloro-4-fluorophenyl)-4-oxo-1,4-dihydro-1,8-naphthyridine-3-carboxamide (**41**)

Yellow solid, yield: 61.5%; m. p.: 214.3–215.1 °C; ^{1}H NMR (400 MHz, DMSO-d_6) δ 12.22 (s, 1H), 12.13 (s, 1H), 8.91 (s, 1H), 8.83 (d, *J* = 7.8 Hz, 2H), 8.31 (s, 1H), 7.83 (d, *J* = 8.7 Hz, 2H), 7.70 (d, *J* = 8.5 Hz, 5H), 7.47 (s, 1H), 7.28 (d, *J* = 8.4 Hz, 2H), 6.49 (s, 1H). Anal. calcd. for $C_{27}H_{15}ClF_2N_6O_3$ (%): C, 59.51; H, 2.77; Cl, 6.51; F, 6.97; N, 15.42; Found (%): C, 59.50; H, 2.76; N, 15,43. ESI-MS: *m/z* 544.1 $[M+H]^+$.

4.3.31. N-(4-((7H-pyrrolo[2,3-d]pyrimidin-4-yl)oxy)-3-fluorophenyl)-1-(4-methoxyphenyl)-4-oxo-1,4-dihydro-1,8-naphthyridine-3-carboxamide (**42**)

Yellow solid, yield: 65.5%; m. p.: 212.3–215.6 °C; ^{1}H NMR (400 MHz, DMSO-d_6) δ 12.32 (s, 1H), 12.29 (s, 1H), 8.87 (s, 1H), 8.84 (s, 2H), 8.31 (s, 1H), 7.98 (s, 1H), 7.57 (s, 2H), 7.52 (s, 3H), 7.45 (s, 1H), 7.16 (d, *J* = 8.2 Hz, 2H), 6.62 (s, 1H), 3.87 (s, 3H). ^{13}C NMR (100 MHz, DMSO-d_6) δ 176.94, 161.64, 160.85, 156.05, 154.00, 153.54, 149.98, 149.46, 149.20, 136.84, 136.79, 136.02, 135.13, 131.23, 128.61, 127.07, 127.02, 125.57, 124.64, 122.40, 121.07, 119.79, 116.13, 112.47, 108.30, 104.02, 97.73, 58.98. Anal. calcd. for $C_{28}H_{19}FN_6O_4$ (%): C, 64.37; H, 3.67; F, 3.64; N, 16.08; Found (%): C, 64.36; H, 3.68; N, 16.09. ESI-MS: *m/z* 522.1 $[M+H]^+$.

4.3.32. N-(4-((7H-pyrrolo[2,3-d]pyrimidin-4-yl)oxy)-3-fluorophenyl)-1-(2-chloro-4-(trifluoromethyl)phenyl)-4-oxo-1,4-dihydro-1,8-naphthyridine-3-carboxamide (**43**)

Yellow solid, yield: 55.7%; m. p.: 211.1–213.4 °C; ^{1}H NMR (400 MHz, DMSO-d_6) δ 12.31 (s, 1H), 12.13 (s, 1H), 9.06 (s, 1H), 8.83 (d, *J* = 7.9 Hz, 2H), 8.31 (s, 1H), 8.01 (br, 2H), 7.83 (br, 3H), 7.52 (s, 2H), 7.45 (t, *J* = 8.8 Hz, 1H), 6.62 (s, 1H). ^{13}C NMR (100 MHz, DMSO-d_6) δ 177.48, 162.17, 161.37, 158.89, 155.21 (d, *J* = 229 Hz), 154.58, 153.10, 150.49, 149.96, 149.75, 137.34 (d, *J* = 10 Hz), 136.59, 135.76 (d, *J* = 12 Hz), 131.76, 128.35 (d, *J* = 154 Hz), 126.06, 125.19, 123.86, 122.94, 121.62, 120.51, 120.28, 116.68, 113.05, 108.94, 108.71, 104.55, 98.30. Anal. calcd. for $C_{28}H_{15}ClF_4N_6O_3$ (%): C, 56.53; H, 2.54; Cl, 5.96; F, 12.77; N, 14.13; Found (%): C, 56.53; H, 2.55; N, 14.14. ESI-MS: *m/z* 594.1 $[M+H]^+$.

4.3.33. N-(4-((7H-pyrrolo[2,3-d]pyrimidin-4-yl)oxy)phenyl)-4-oxo-1-phenyl-1,4-dihydro-1,8-naphthyridine-3-carboxamide (**44**)

Yellow solid, yield: 64.2%; m. p.: 198.1–201.5 °C; ^{1}H NMR (400 MHz, DMSO-d_6) δ 12.22 (s, 1H), 12.16 (s, 1H), 8.86 (d, *J* = 8.6 Hz, 4H), 8.31 (s, 1H), 7.83 (d, *J* = 8.9 Hz, 2H), 7.67 (s, 2H), 7.64 (s, 1H), 7.63 (s, 2H), 7.47 (s, 1H), 7.28 (s, 2H), 6.48 (s, 1H). Anal. calcd. for $C_{27}H_{18}N_6O_3$ (%): C, 68.35; H, 3.82; N, 17.71; Found (%): C, 68.34; H, 3.81; N, 17.70. ESI-MS: *m/z* 474.1 $[M+H]^+$.

4.3.34. N-(4-((7H-pyrrolo[2,3-d]pyrimidin-4-yl)oxy)phenyl)-1-(4-bromo-2-fluorophenyl)-4-oxo-1,4-dihydro-1,8-naphthyridine-3-carboxamide (**45**)

Yellow solid, yield: 51.5%; m. p.: 223.3–224.6 °C; ^{1}H NMR (400 MHz, DMSO-d_6) δ 12.02 (s, 1H), 9.04 (s, 1H), 8.85 (s, 1H), 8.64 (s, 2H), 8.45 (s, 1H), 8.29 (s, 1H), 7.94 (s, 2H), 7.81 (s, 2H), 7.73 (s, 1H), 7.66 (s, 1H), 7.47 (s, 1H), 7.28 (d, *J* = 8.6 Hz, 2H). Anal. calcd. for $C_{27}H_{16}BrFN_6O_3$ (%): C, 56.76; H, 2.82; Br, 13.98; F, 3.33; N, 14.71; Found (%): C, 56.75; H, 2.81; N, 14.70. ESI-MS: *m/z* 570.0 $[M+H]^+$.

4.3.35. N-(4-((7H-pyrrolo[2,3-d]pyrimidin-4-yl)oxy)phenyl)-1-(4-bromophenyl)-4-oxo-1,4-dihydro-1,8-naphthyridine-3-carboxamide(**46**)

Yellow solid, yield: 50.6%; m. p.: 245.3–246.1 °C; ^{1}H NMR (400 MHz, DMSO-d_6) δ 12.13 (s, 1H), 8.91 (s, 1H), 8.81 (s, 1H), 8.30 (s, 1H), 7.84 (d, *J* = 6.8 Hz, 5H), 7.67 (t, *J* = 8.3 Hz, 4H), 7.47 (s, 1H), 7.28 (d, *J* = 8.4 Hz, 2H), 6.48 (s, 1H). ^{13}C NMR (100 MHz, DMSO-d_6) δ 176.86, 170.03, 161.67, 161.56, 153.62, 153.51, 150.08, 149.72, 148.94, 148.42, 139.63, 135.89, 135.59, 132.32 (2C), 130.02 (2C), 125.24, 122.53 (2C), 122.04, 121.31, 120.83 (2C), 112.03, 104.57, 97.96. Anal. calcd. for $C_{27}H_{17}BrN_6O_3$ (%): C, 58.60; H, 3.10; Br, 14.44; N, 15.19; Found (%): C, 58.61; H, 3.11; N, 15.18. ESI-MS: *m/z* 552.1 $[M+H]^+$.

*4.3.36. N-(4-((7H-pyrrolo[2,3-d]pyrimidin-4-yl)oxy)phenyl)-1-(4-chlorophenyl)-4-oxo-1,4-dihydro-1,8-naphthyridine-3-carboxamide (**47**)*

Yellow solid, yield: 43.5%; m. p.: 213.4–215.5 °C; ^{1}H NMR (400 MHz, DMSO-d_6) δ 12.22 (s, 1H), 12.13 (s, 1H), 8.91 (s, 1H), 8.83 (d, J = 7.8 Hz, 2H), 8.31 (s, 1H), 7.83 (d, J = 8.7 Hz, 2H), 7.70 (d, J = 7.5 Hz, 5H), 7.47 (s, 1H), 7.28 (d, J = 8.4 Hz, 2H), 6.49 (s, 1H). Anal. calcd. for $C_{27}H_{17}ClN_6O_3$ (%): C, 63.72; H, 3.37; Cl, 6.97; N, 16.51; Found (%): C, 63.71; H, 3.38; N, 16.53. ESI-MS: m/z 508.1 [M+H] $^+$.

*4.3.37. N-(4-((7H-pyrrolo[2,3-d]pyrimidin-4-yl)oxy)phenyl)-1-(4-fluorophenyl)-4-oxo-1,4-dihydro-1,8-naphthyridine-3-carboxamide (**48**)*

Yellow solid, yield: 45.1%; m. p.: 220.3–221.3 °C; ^{1}H NMR (400 MHz, DMSO-d_6) δ 12.22 (s, 1H), 12.15 (s, 1H), 8.90 (s, 1H), 8.82 (s, 1H), 8.49 (s, 1H), 8.31 (s, 1H), 7.83 (d, J = 9.0 Hz, 2H), 7.75 (s, 2H), 7.47 (br, 4H), 7.28 (d, J = 8.5 Hz, 2H). Anal. calcd. for $C_{27}H_{17}FN_6O_3$ (%): C, 65.85; H, 3.48; F, 3.86; N, 17.07; Found (%): C, 65.84; H, 3.47; N, 17.06. ESI-MS: m/z 492.1 [M+H] $^+$.

*4.3.38. N-(4-((7H-pyrrolo[2,3-d]pyrimidin-4-yl)oxy)phenyl)-1-(3-chloro-4-fluorophenyl)-4-oxo-1,4-dihydro-1,8-naphthyridine-3-carboxamide (**49**)*

Yellow solid, yield: 44.8%; m. p.: 204.3–206.9 °C; ^{1}H NMR (400 MHz, DMSO-d_6) δ 12.22 (s, 1H), δ 12.11 (s, 1H), 8.96 (s, 1H), 8.84 (s, 1H), 8.76 (s, 1H), 8.65 (s, 1H), 8.31 (s, 2H), 7.84 (s, 3H), 7.74 (br, 2H), 7.66 (s, 1H), 7.30 (s, 2H). Anal. calcd. for $C_{27}H_{16}ClFN_6O_3$ (%): C, 61.55; H, 3.06; Cl, 6.73; F, 3.61; N, 15.95; Found (%): C, 61.54; H, 3.07; N, 15.96. ESI-MS: m/z 526.1 [M+H] $^+$.

*4.3.39. N-(4-((7H-pyrrolo[2,3-d]pyrimidin-4-yl)oxy)phenyl)-1-(4-methoxyphenyl)-4-oxo-1,4-dihydro-1,8-naphthyridine-3-carboxamide (**50**)*

Yellow solid, yield: 46.3%; m. p.: 222.8–225.6 °C; ^{1}H NMR (400 MHz, DMSO-d_6) δ 12.24 (s, 1H), 12.17 (s, 1H), 8.87 (s, 1H), 8.82 (s, 2H), 8.31 (s, 1H), 7.82 (d, J = 9.0 Hz, 2H), 7.58 (d, J = 9.1 Hz, 3H), 7.48 (s, 1H), 7.28 (d, J = 9.0 Hz, 2H), 7.16 (d, J = 9.0 Hz, 2H), 3.87 (s, 3H). ^{13}C NMR (100 MHz, DMSO-d_6) δ 177.29, 162.22, 160.07, 154.14, 154.03, 150.89, 150.62, 149.88, 148.98, 136.34, 136.15, 133.76, 129.33 (2C), 125.66, 123.01 (2C), 122.41, 121.91, 121.42, 121.35 (2C), 114.98 (2C), 112.29, 105.09, 98.49, 56.06. Anal. calcd. for $C_{28}H_{20}N_6O_4$ (%): C, 66.66; H, 4.00; N, 16.66; Found (%): C, 66.67; H, 4.02; N, 16.68. ESI-MS: m/z 504.2 [M+H] $^+$.

*4.3.40. N-(4-((7H-pyrrolo[2,3-d]pyrimidin-4-yl)oxy)phenyl)-1-(2-chloro-4-(trifluoromethyl)phenyl)-4-oxo-1,4-dihydro-1,8-naphthyridine-3-carboxamide (**51**)*

Yellow solid, yield: 43.9%; m. p.: 212.6–215.9 °C; ^{1}H NMR (400 MHz, DMSO-d_6) δ 12.22 (s, 1H), 12.02 (s, 1H), 9.04 (s, 1H), 8.84 (s, 2H), 8.31 (s, 1H), 7.94 (s, 1H), 7.82 (d, J = 8.7 Hz, 3H), 7.72 (s, 2H), 7.47 (s, 2H), 7.28 (d, J = 8.7 Hz, 2H). ^{13}C NMR (100 MHz, DMSO-d_6) δ 177.48, 162.16, 161.38, 158.89, 156.36, 155.54, 154.56, 154.09, 150.49, 149.94, 136.58, 131.76, 128.34 (d, J = 153 Hz), 126.04, 125.18, 123.76, 122.91 (2C), 121.62, 120.51, 116.66 (2C), 113.07 (2C), 108.94, 108.71, 104.57. Anal. calcd. for $C_{28}H_{16}ClF_3N_6O_3$ (%): C, 58.29; H, 2.80; Cl, 6.14; F, 9.88; N, 14.57; Found (%): C, 58.28; H, 2.81; N, 14.56. ESI-MS: m/z 576.1 [M+H] $^+$.

4.4. MTT assay in vitro

The cytotoxic activities of target compounds **20**–**51** were evaluated with A549, Hela and MCF-7 cell lines using the standard MTT assay with Cabozantinib as the positive control. First, approximately 6 × 10^3 cells suspended in a minimum essential medium (MEM) were plated onto each well in a 96-well plate and were incubated in 5% CO_2 at 37 °C for 24 h. Next, the cancer cell lines adding test compounds at concentrations of 1.234, 3.704, 11.11, 33.33 and 100 μmol/L were continued for 72 h in 5% CO_2 at 37 °C. Afterward, fresh MTT was added to each well at a terminal concentration of 5 g/mL and was incubated with cells at 37 °C for 4 h. Finally, after the removal of MTT methoxypyrimidine, the cells were dissolved in 100 μL dimethyl sulfoxide, and the data were recorded under an absorbance of 492 nm. All compounds were tested three times under the same conditions, and the test results were expressed by IC_{50} with the Bacus Laboratories Incorporated Slide Scanner (Bliss) software.

4.5. Cell apoptosis assay by flow cytometry

A549 cells were seeded in 6-well plates at a density of 1 × 10^6 cells/well in RPMI 1640 medium and were incubated for 24 h. The cancer cell lines were then treated with 0.5 μM Cabozantinib and compound **51** for 48 h at 37 °C in 5% CO_2. Cultured cells stained with Annexin V-FITC and propidium iodide (PI) at 4 °C for 0.5 h were tested using the FACS Calibur flow cytometer (Becton Dickinson, San Jose, CA) by the Cell Quest software in the dark.

4.6. Tyrosine kinases assays

First, the kinase buffer base was prepared with configured 0.0015% Brij-35 at 50 mM HEPES (pH = 7.5). Additionally, all compounds were diluted to five concentrations using 100% DMSO. A new solution consisting of the above dissolved compound along with the kinase buffer group was added to the 96-well plate and shaken under r. t. for 10 min. The mixture in the 96-well plates was then transferred in duplicate to 384-well plates, and 10 μL of enzyme solution was added to each 384-well assay plate. After incubating at r. t. for 10 min, the 2.5x peptide solution (10 μL) formed by adding FAM-labeled peptide and ATP to the kinase base buffer was added to each well on the plates. Stop buffer was added to stop the reaction after incubating for a certain period at 28 °C. The final result was obtained by the caliper collecting the data and copying the conversion data, after which it further converted the data to the inhibition value. The correspondingly obtained formula was: percent inhibition = (max-conversion)/(max-min)*100. Here, “max” stands for DMSO control, while “min” stands for low control [35,36].

Declaration of competing interest

The authors declare that they have no known competing financial interests or personal relationships that could have appeared to influence the work reported in this paper.

Acknowledgments

We gratefully acknowledge the generous support provided by The National Natural Science Foundation of China (No. 81660572), and Natural Science Foundation of Jiangxi, China (No. 20192ACBL21009).

References

[1] R.L. Siegel, K.D. Miller, A. Jemal, Cancer statistics, 2019, CA, Cancer J. Clin. 69 (2019) 7–34.
[2] K.D. Miller, L. Nogueira, A.B. Mariotto, J.H. Rowland, K.R. Yabroff, C.M. Alfano, A. Jemal, J.L. Kramer, R.L. Siegel, Cancer treatment and survivorship statistics, 2019, CA, Cancer J. Clin. 69 (2019) 363–385.
[3] J. Ferlay, M. Colombet, I. Soerjomataram, C. Mathers, D.M. Parkin, M. Pineros, A. Znaor, F. Bray, Estimating the global cancer incidence and mortality in 2018: GLOBOCAN sources and methods, Int. J. Canc. 144 (2019) 1941–1953.
[4] D. Chen, C.K. Soh, W.H. Goh, H. Wang, Design, synthesis, and preclinical

evaluation of fused pyrimidine-based hydroxamates for the treatment of hepatocellular carcinoma, J. Med. Chem. 61 (2018) 1552–1575.
[5] J. Zugazagoitia, C. Guedes, S. Ponce, I. Ferrer, S. Molina-Pinelo, L. Paz-Ares, Current challenges in cancer treatment, Clin. Therapeut. 38 (2016) 1551–1566.
[6] H.B. El-Serag, Hepatocellular carcinoma: an epidemiologic view, J. Clin. Gastroenterol. 35 (2002) S72–S78.
[7] P. Blume-Jensen, T. Hunter, Oncogenic kinase signalling, Nature 411 (2001) 355–365.
[8] S.A. Kaliberov, D.J. Buchsbaum, Chapter seven–Cancer treatment with gene therapy and radiation therapy, Adv. Canc. Res. 115 (2012) 221–263.
[9] F. Cecchi, D.C. Rabe, D.P. Bottaro, Targeting the HGF/Met signaling pathway in cancer therapy, Expert Opin. Ther. Targets 16 (2012) 553–572.
[10] D.G.F. Al-U'datt, B.A.A. Al-Husein, G.R. Qasaimeh, A mini-review of c-Met as a potential therapeutic target in melanoma, Biomed. Pharmacother. 88 (2017) 194–202.
[11] A. Fafalios, J. Ma, X. Tan, J. Stoops, J. Luo, M.C. Defrances, R. Zarnegar, A hepatocyte growth factor receptor (Met)-insulin receptor hybrid governs hepatic glucose metabolism, Nat. Med. 17 (2011) 1577–1584.
[12] M.V. Karamouzis, P.A. Konstantinopoulos, A.G. Papavassiliou, Targeting MET as a strategy to overcome crosstalk-related resistance to EGFR inhibitors, Lancet Oncol. 10 (2009) 709–717.
[13] C.M. Stellrecht, V. Gandhi, MET receptor tyrosine kinase as a therapeutic anticancer target, Canc. Lett. 280 (2009) 1–14.
[14] A. Danilkovitch-Miagkova, B. Zbar, Dysregulation of Met receptor tyrosine kinase activity in invasive tumors, J. Clin. Invest. 109 (2002) 863–867.
[15] Q. Tang, Y. Duan, L. Wang, M. Wang, Y. Ouyang, C. Wang, H. Mei, S. Tang, Y. Xiong, P. Zheng, P. Gong, W. Zhu, Synthesis and antiproliferative activity of pyrrolo[2,3-*b*]pyridine derivatives bearing the 1,8-naphthyridin-2-one moiety, Eur. J. Med. Chem. 143 (2018) 266–275.
[16] S. Berthou, D.M. Aebersold, L.S. Schmidt, D. Stroka, C. Heigl, B. Streit, D. Stalder, G. Gruber, C. Liang, A.R. Howlett, D. Candinas, R.H. Greiner, K.E. Lipson, Y. Zimmer, The Met kinase inhibitor SU11274 exhibits a selective inhibition pattern toward different receptor mutated variants, Oncogene 23 (2004) 5387–5393.
[17] M.H. Norman, L. Liu, M. Lee, N. Xi, I. Fellows, N.D. D'Angelo, C. Dominguez, K. Rex, S.F. Bellon, T.S. Kim, I. Dussault, Structure-based design of novel class II c-Met inhibitors: 1. Identification of pyrazolone-based derivatives, J. Med. Chem. 55 (2012) 1858–1867.
[18] J.J. Cui, Targeting receptor tyrosine kinase MET in cancer: small molecule inhibitors and clinical progress, J. Med. Chem. 57 (2014) 4427–4453.
[19] F. Bentzien, M. Zuzow, N. Heald, A. Gibson, Y. Shi, L. Goon, P. Yu, S. Engst, W. Zhang, D. Huang, L. Zhao, V. Vysotskaia, F. Chu, R. Bautista, B. Cancilla, P. Lamb, A.H. Joly, F.M. Yakes, *In vitro* and *in vivo* activity of cabozantinib (XL184), an inhibitor of RET, MET, and VEGFR2, in a model of medullary thyroid cancer, Thyroid 23 (2013) 1569–1577.
[20] M.S. Wang, L.S. Zhuo, F.P. Yang, W.J. Wang, W. Huang, G.F. Yang, Synthesis and biological evaluation of new MET inhibitors with 1,6-naphthyridinone scaffold, Eur. J. Med. Chem. 185 (2020) 111803.
[21] Y. Huang, S.F. Lu, C.J. Hu, S.P. Fu, W.X. Shen, W.X. Liu, Q. Li, N. Wang, S.Y. He, F.R. Liang, B.M. Zhu, Electro-acupuncture at Neiguan pretreatment alters genome-wide gene expressions and protects rat myocardium against ischemia-reperfusion, Molecules 19 (2014) 16158–16178.
[22] Q. Xu, B. Dai, Z. Li, L. Xu, D. Yang, P. Gong, Y. Hou, Y. Liu, Design, synthesis, and biological evaluation of 4-((6,7-dimethoxyquinoline-4-yl)oxy)aniline derivatives as FLT3 inhibitors for the treatment of acute myeloid leukemia, Bioorg. Med. Chem. Lett 29 (2019) 126630.
[23] L. Wang, X. Liu, S. Xu, Q. Tang, Y. Duan, Z. Xiao, J. Zhi, L. Jiang, P. Zheng, W. Zhu, Discovery of novel pyrrolo-pyridine/pyrimidine derivatives bearing pyridazinone moiety as c-Met kinase inhibitors, Eur. J. Med. Chem. 141 (2017) 538–551.
[24] G. Argiropoulos, M.R. Bates, P. Cherubim, L.W. Deady, A.M. Ganakas, B.C. Baguley, W.A. Denny, Cytotoxic and DNA binding properties of aminoalkyl derivatives of di- and triazaphenanthrenes, Anticancer Drug Des 7 (1992) 285–296.
[25] U. Hoch, J. Lynch, Y. Sato, S. Kashimoto, F. Kajikawa, Y. Furutani, J.A. Silverman, Voreloxin, formerly SNS-595, has potent activity against a broad panel of cancer cell lines and *in vivo* tumor models, Canc. Chemother. Pharmacol. 64 (2009) 53–65.
[26] X.L. Zhao, C.Z. Yu, Vosaroxin induces mitochondrial dysfunction and apoptosis in cervical cancer HeLa cells: involvement of AMPK/Sirt3/HIF-1 pathway, Chem. Biol. Interact. 290 (2018) 57–63.
[27] Y. Xu, N.Y. Wang, X.J. Song, Q. Lei, T.H. Ye, X.Y. You, W.Q. Zuo, Y. Xia, L.D. Zhang, L.T. Yu, Discovery of novel *N*-(5-(tert-butyl)isoxazol-3-yl)-*N'*-phenylurea analogs as potent FLT3 inhibitors and evaluation of their activity against acute myeloid leukemia *in vitro* and *in vivo*, Bioorg. Med. Chem. Lett 23 (2015) 4333–4343.
[28] H. Yang, N. Huo, P. Yang, H. Pei, H. Lv, X. Zhang, Rhodium catalyzed asymmetric hydrogenation of 2-pyridine ketones, Org. Lett. 17 (2015) 4144–4147.
[29] Z. Chen, M. Ning, Q. Zou, H. Cao, Y. Ye, Y. Leng, J. Shen, Discovery and structure-activity relationship study of 4-Phenoxythiazol-5-carboxamides as highly potent TGR5 agonists, Chem. Pharm. Bull. 64 (2016) 326–339.
[30] H. Yuan, Q. Liu, L. Zhang, S. Hu, T. Chen, H. Li, Y. Chen, Y. Xu, T. Lu, Discovery, optimization and biological evaluation for novel c-Met kinase inhibitors, Eur. J. Med. Chem. 143 (2018) 491–502.
[31] H. Hu, F. Chen, Y. Dong, M. Li, S. Xu, M. Qin, P. Gong, Discovery of Novel c-Mesenchymal-Epithelia transition factor and histone deacetylase dual inhibitors, Eur. J. Med. Chem. 204 (2020) 112651.
[32] J.F. Wu, M.M. Liu, S.X. Huang, Y. Wang, Design and synthesis of novel substituted naphthyridines as potential c-Met kinase inhibitors based on MK-2461, Bioorg. Med. Chem. Lett 25 (2015) 3251–3255.
[33] M.J. Li, G.Z. Wu, Q. Kaas, T. Jiang, R.L. Yu, Development of efficient docking strategies and structure-activity relationship study of the c-Met type II inhibitors, J. Mol. Graph. Model. 75 (2017) 241–249.
[34] H. Yuan, J. Zhuang, S. Hu, H. Li, J. Xu, Y. Hu, X. Xiong, Y. Chen, T. Lu, Molecular modeling of exquisitely selective c-Met inhibitors through 3D-QSAR and molecular dynamics simulations, J. Chem. Inf. Model. 54 (2014) 2544–2554.
[35] L. Liu, A. Siegmund, N. Xi, P. Kaplan-Lefko, K. Rex, A. Chen, J.J. Lin, L. Moriguchi, L. Berry, Y. Huang, Y. Teffera, Y. Yang, S.F. Zhang, M. Bellon, R. Lee, A. Shimanovich, C. Bak, M.H. Dominguez, J.C. Norman, I. Harmange, T.S. Dussault, Kim, Discovery of a potent, selective, and orally bioavailable c-Met inhibitor: 1-(2-hydroxy-2-methylpropyl)-*N*-(5-(7-methoxyquinolin-4-yloxy)pyridin-2-yl)-5-methyl-3-oxo-2-phenyl-2,3-dihydro-1*H*-pyrazole-4-carboxamide (AMG 458), J. Med. Chem. 51 (2008) 3688–3691.
[36] M.L. Peach, N. Tan, S.J. Choyke, A. Giubellino, G. Athauda, T.R. Burke, r. J, M.C. Nicklaus, D.P. Bottaro, Directed discovery of agents targeting the Met tyrosine kinase domain by virtual screening, J. Med. Chem. 52 (2009) 943–951.